Journal of the Korean Crystal Growth and Crystal Technology
Vol. 33, No. 4 (2023) 132-138
https://doi.org/10.6111/JKCGCT.2022.33.4.132

p-ISSN 1225-1429
e-ISSN 2234-5078

Enhanced photocatalytic performance of magnesium-lithium co-doped $BiVO_4$ and its degradation of methylene blue

Nayoung Kim, Hyeonjin Kim, Jiyu Lee and Seog-Young Yoon†

School of Materials Science and Engineering, Pusan National University, Pusan 46241, Korea

(Received June 5, 2023)
(Revised June 21, 2023)
(Accepted June 29, 2023)

Abstract Doped and undoped-$BiVO_4$ samples with different elements (Li, Mg) and amounts were synthesized with a hydrothermal method. The synthesized samples were characterized using various techniques including X-ray diffraction (XRD), X-ray photoelectron spectroscopy (XPS), UV-Vis diffusion reflectance spectroscopy (UV-Vis DRS), and photoluminescence (PL) spectroscopy. Photocatalytic activity of the samples was evaluated by measuring the degradation of methyl blue (MB) under visible light irradiation. The results indicated that the incorporation of Mg and Li into $BiVO_4$ caused lattice distortion, the presence of surface hydroxyl groups, a narrower band gap, and a reduced recombination ratio of photo-induced electron-hole pairs. Notably, the photocatalytic activity of Mg5%–Li5% co-doped $BiVO_4$ sample exhibited a significant improvement compared to that of undoped $BiVO_4$ sample.

Key words $BiVO_4$, Photocatalytic activity, Co-doping, Energy band gap, Electron-hole recombination

1. Introduction

The environmental pollution and energy crisis, resulting from rapid industrialization, have led to problems that mankind must solve. To address these problems, using semiconductor materials as photo-catalysts has been recognized as a cost-effective approach for the degradation of organic pollutants into harmless chemicals, and split water to generate hydrogen for fuel [1-3]. Typical photocatalytic metal oxide semiconductors are TiO_2, $BiVO_4$, Bi_2O_3, etc. To date, extensive research has been conducted on TiO_2 based catalysts. However, TiO_2 can only absorb ultraviolet light ($\lambda < 400$ nm) due to its large energy band gap of 3.2 eV, making it unsuitable for visible light-assisted photocatalytic oxidation [4,5]. $BiVO_4$ has a narrower energy band gap (2.4 eV), making it an ideal photocatalytic semiconductor for pollutant degradation and solar fuel generation via water splitting under irradiation with visible light. Moreover, it has the advantages of being inexpensive, non-toxic, and chemically stable, resistant to photo-corrosion. However, $BiVO_4$ is limited in its use as a photocatalyst because of a low interfacial charge transfer rate caused by a low quantum efficiency and a high photo-produced electron-hole pairs recombination ratio [6-8]. The main factors influencing photocatalytic efficiency include the energy band gap, charge carrier mobility, and electron-hole recombination rate. To enhance photocatalytic performance, metal doping [9] is commonly used as it significantly increases the concentration and mobility of charge carriers. Metal doping also contributes to the creation of impurity energy states and new states within the band gap [10,11]. Metal doped $BiVO_4$ has been synthesized using various methods, including solid-state reactions, co-precipitation, the sol-gel method, and the hydrothermal method. The hydrothermal method is a low temperature synthesis method that offers good composition control and is suitable for high purity chemical processes [12,13].

In this study, we synthesized undoped $BiVO_4$, Mg-doped $BiVO_4$, Li-doped $BiVO_4$, and Mg-Li co-doped $BiVO_4$ using a hydrothermal method. These samples were then characterized to investigate the impact of Mg-Li co-doping on photocatalytic activity. X-ray diffraction (XRD), X-ray photoelectron spectroscopy (XPS), UV-Vis diffusion reflectance (DRS) spectroscopy, and photoluminescence (PL) spectroscopy were employed to characterize the samples. Photocatalytic activity was evaluated by measuring the degradation of methyl blue (MB) through photodegradation under irradiation with visible light.

†Corresponding author
E-mail: syy3@pusan.ac.kr

2. Materials and Methods

2.1. Powder preparation

$Bi(NO_3)_3 \cdot 5H_2O$ (Junsei, 98 %), NH_4VO_3 (Junsei, 99 %), $LiNO_3$ (Junsei, 98 %), $Mg(NO_3)_2 \cdot 6H_2O$ (Samchun, 98 %), ammonia water, and distilled water were utilized in the experiment. The co-precipitation and hydrothermal method was used to synthesize monoclinic scheelite $BiVO_4$ (bismuth(III) vanadate) samples.

The $BiVO_4$ powder was prepared as follows: First, an aqueous solution of NH_4VO_3 (0.1 M) was co-precipitated into an aqueous solution of $Bi(NO_3)_3 \cdot 5H_2O$ (0.1 M) at pH 11, maintained by the addition of ammonia water. The resulting mixture was subjected to the hydrothermal process by heating it to 200°C for 15 h, resulting in the formation of a yellow precipitate. The precipitate was filtered with distilled water several times to remove any remaining impurities, and subsequently dried in an oven at 80°C for 24 h. The same method was followed for the preparation of $BiVO_4$ samples doped with Mg (5, 7.5 mol%), Li (5, 7.5 mol%), and Mg-Li (5-5, 5-7.5, 7.5-5, 7.5-7.5 mol%).

2.2. Characterization

The crystallinity and phase purity of the samples were evaluated using X-ray diffraction with Cu Kα radiation (UltimaIV, Rigaku). The X-ray diffraction measurements were conducted with an accelerating voltage of 40 kV and an applied current of 40 mA. The Rietveld refinement method was used to characterize structural analysis. X-ray photoelectron spectroscopy (K-ALPHA+XPS System, Thermo Fisher Scientific) was used to analyze the chemical states of the prepared samples. UV-Vis-NIR spectrophotometer (V670, JASCO) was used to collect UV-Vis diffuse reflectance spectra. Photoluminescence emission spectra were obtained using photoluminescence spectroscopy (Spectrograph 500i, Acton Research) at room temperature. The methyl blue dye in a photo-reactor by using a UV irradiation (λ = 405 nm, 50 W) was examined to evaluate the photocatalytic performance of the samples.

2.3. Photocatalytic activity test

In a typical photo-degradation experiment, a suspension of 50 mL aqueous solution of MB (20 ppm) mixed with 0.1 g of sample was magnetically stirred in the dark for 30 min. The photocatalytic activity was tested at 405 nm irradiation (50 W, Philips). At 30 min intervals of irradiation time, aliquots were extracted and the catalyst was removed by centrifugation. UV-Vis-NIR spectroscopy was used to measure the remaining concentration of MB in the aliquots.

3. Results and Discussion

3.1. XRD analysis

Figure 1 presents the XRD patterns of the prepared $BiVO_4$ samples with varying dopant contents. The diffraction peaks of all $BiVO_4$ samples were identified as belonging to monoclinic $BiVO_4$ (ICDD No. 00-014-0688), with no extraneous peaks observed.

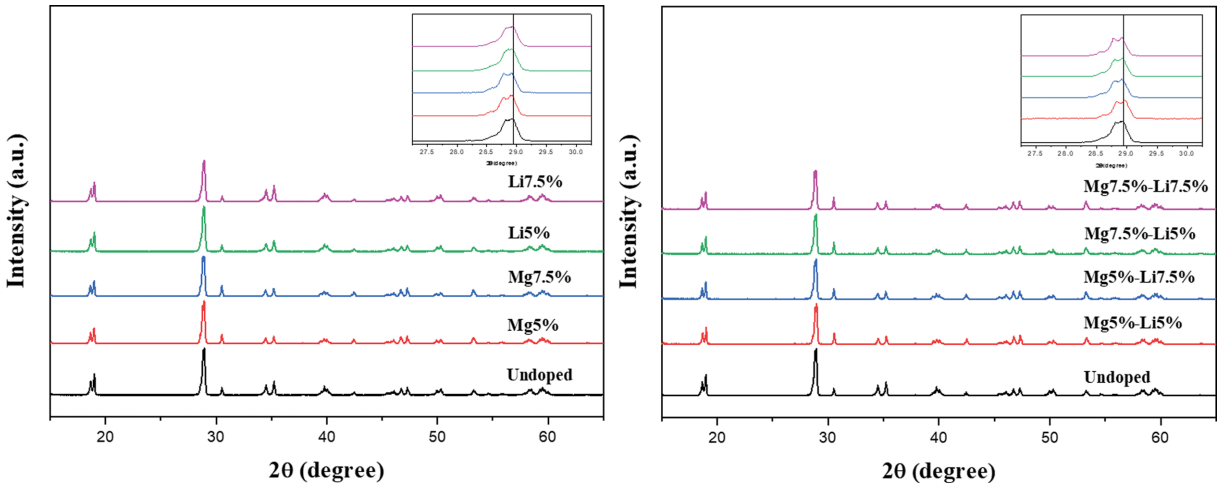

Fig. 1. X-ray diffraction patterns of $BiVO_4$ samples with different doping elements and amounts. The inset shows characteristic peak shift to higher angle 2θ.

Table 1
Lattice parameters and Rietveld refinement results of $BiVO_4$ samples

	a (Å)	b (Å)	c (Å)	α	β	γ	V (Å^3)	χ^2
Undoped	5.1970	11.7040	5.0944	90.0	90.381	90.0	309.87	1.7214
Mg5%	5.2001	11.7120	5.0955	90.0	90.387	90.0	310.33	1.4738
Mg7.5%	5.1992	11.7098	5.0945	90.0	90.387	90.0	310.16	1.5678
Li5%	5.1986	11.7022	5.0939	90.0	90.387	90.0	309.55	1.7595
Li7.5%	5.1980	11.7028	5.0935	90.0	90.379	90.0	309.49	1.9931
Mg5%-Li5%	5.1936	11.697	5.0890	90.0	90.387	90.0	309.15	1.4825
Mg5%-Li7.5%	5.1968	11.7043	5.0922	90.0	90.387	90.0	309.73	1.4834
Mg7.5%-Li5%	5.1948	11.6999	5.090284	90.0	90.387	90.0	309.37	1.5794
Mg7.5%-Li7.5%	5.1982	11.7075	5.0935	90.0	90.387	90.0	309.97	1.5199

The sharp diffraction peaks observed in the samples indicate their high crystallinity, indicating the successful synthesis of all the $BiVO_4$ samples via the hydrothermal method. The variation in intensity and the FWHM in the peaks could be attributed to the disorder in the distribution of metal dopants within the structure [14]. The XRD peaks of the doped samples showed a shift compared to undoped $BiVO_4$, indicating that the monoclinic $BiVO_4$ structure was distorted by metal doping. The Rietveld refinement method was used to analyze the lattice parameters of the $BiVO_4$ samples, as shown in Table 1. In lattice volume, Mg-doped samples increased and Li-doped samples decreased. These results suggest that Mg^{2+} ions (0.72 Å) substituted V^{5+} ions (0.54 Å) and Li^{+} ions (0.92 Å) substituted Bi^{3+} ions (1.17 Å). The lattice parameters and volume of Mg-Li co-doped samples decreased, suggesting that Mg^{2+} and Li^{+} interacted with each other in the lattice. Importantly, Mg5%-Li5% co-doped $BiVO_4$ exhibited the largest variation in lattice parameters.

3.2. XPS analysis

XPS is a valuable technique for the identification of chemical states. Figure 2 shows the XPS spectra of Mg5%-Li5% co-doped $BiVO_4$. Depending on the survey spectra, the sample contained Bi, V, O, Mg, Li, and C elements. The C 1s peak was used as a reference. In Fig. 2(b), the high-resolution XPS spectrum of Bi 4f shows two peaks at binding energies of 158.6 eV (Bi $4f_{5/2}$) and 163.9 eV (Bi $4f_{7/2}$). In Fig. 2(c) V 2p peaks were detected at 516.2 eV (V $2p_{3/2}$)

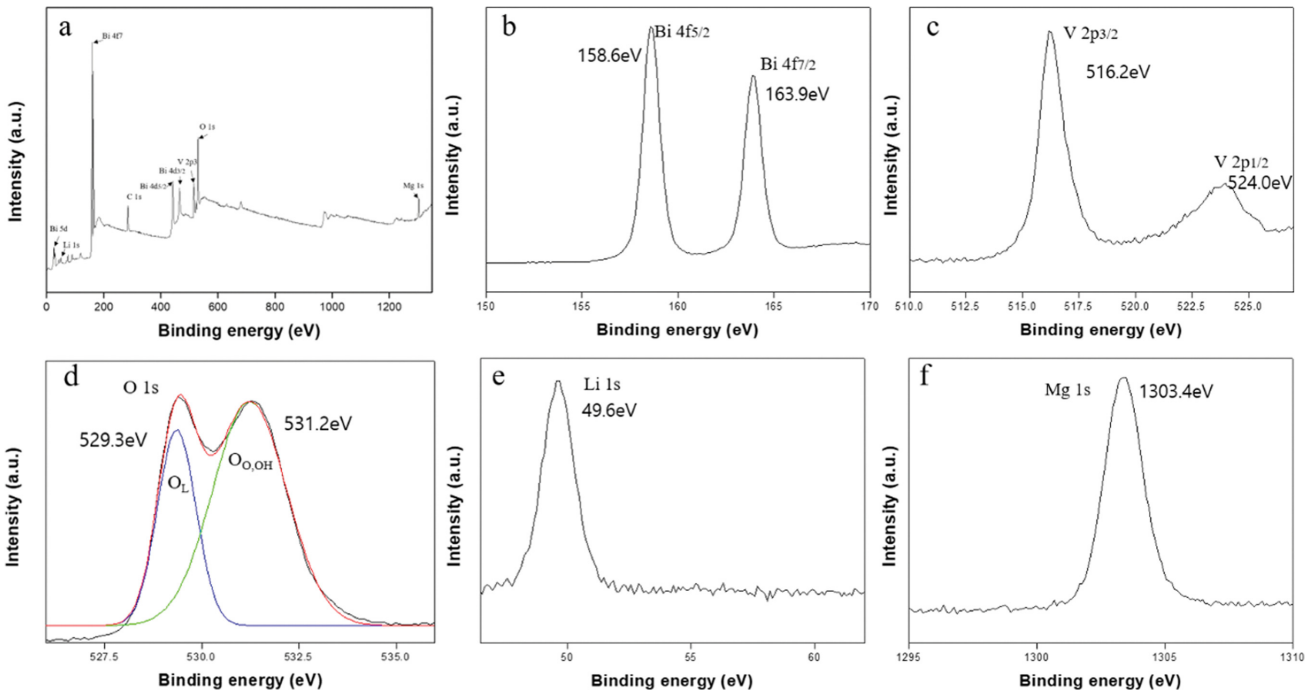

Fig. 2. XPS spectra of Mg5%-Li5% doped sample; (a) survey spectra, (b) Bi 4f, (c) V 2p, (d) O 1s, (e) Li 1s, (f) Mg 1s.

and 524.0 eV (V $2p_{1/2}$). These results indicate that Bi^{3+} and V^{5+} exist in Mg5%-Li5% co-doped $BiVO_4$ [15, 16]. Figure 2(d) shows the O 1s spectrum, which was deconvoluted using Gaussian curve fitting. The peak at 529.3 eV was assigned to lattice oxygen present in Mg5%-Li5% co-doped $BiVO_4$ while the peak at 531.2 eV indicated the presence of surface hydroxyl groups (weakly bonded -O and -OH) [17]. The hydroxyl groups contribute to the trapping of photo-induced electrons and holes, which improves the photocatalytic process [18]. Li 1s and Mg 1s peaks were found at 49.6 eV and 1303.4 eV, respectively.

3.3. Optical analysis

Figure 3 shows the DRS spectra of the synthesized samples. Doped $BiVO_4$ samples exhibited an enhanced ability to absorb visible light. In comparison to the undoped $BiVO_4$, the spectra of the doped samples exhibited a spectral redshift from 500 nm to 530 nm, meaning their photocatalytic active wavelength range had been extended. Tauc's equation was used to calculate the band gap energies (Table 2) of the $BiVO_4$ samples from the UV-Vis spectra [19]:

$$(\propto h\nu)^n = A(h\nu - E_g) \quad (1)$$

In the Tauc's equation, the band gap energy (E_g) is calculated using the absorption coefficient (α), where A is a constant dependent on the transition probability, hv represents the photon energy, and n is a parameter indicating the type of transition (n = 1/2 for indirect and n = 2 for direct transitions). Monoclinic $BiVO_4$ is an indirect band gap semiconductor (n = 1/2) [20-23]. E_g was determined by extrapolating a straight line to the $(\alpha h\nu)^2 = 0$ axis in a plot of $(\alpha h\nu)^2$ versus hv. The doped $BiVO_4$ samples exhibited lower band gap energies compared to the undoped $BiVO_4$. Consequently, the introduction of Mg-Li doping in $BiVO_4$ leads to a decrease in its optical band gap energy. Such doping can induce variations in lattice parameters, potentially leading to the creation of impurity states and new states within the band gap [24,25]. This can introduce the increasing of carrier density, narrow band gap, and enhanced absorption. It is noteworthy that the band gap energies of Mg5%-Li5% co-doped $BiVO_4$ decreased to a greater extent compared to the other doped samples.

Table 2
Energy band gap values from Tauc's equation

	Energy band gap
Undoped	2.435 eV
Mg5%	2.370 eV
Mg7.5%	2.367 eV
Li5%	2.410 eV
Li7.5%	2.415 eV
Mg5%-Li5%	2.348 eV
Mg5%-Li7.5%	2.364 eV
Mg7.5%-Li5%	2.363 eV
Mg7.5%-Li7.5%	2.355 eV

3.4. Photoluminescence emission spectra

Photoluminescence refers to the emission of light that occurs following the absorption of photons. PL emission spectra are generated from the charge carrier transfer, immigration, trapping, and photo-induced electron-hole pairs recombination. Thus, it is useful to use PL emission spectra to investigate the ability of photo-induced electron-hole pair separation [26]. A low

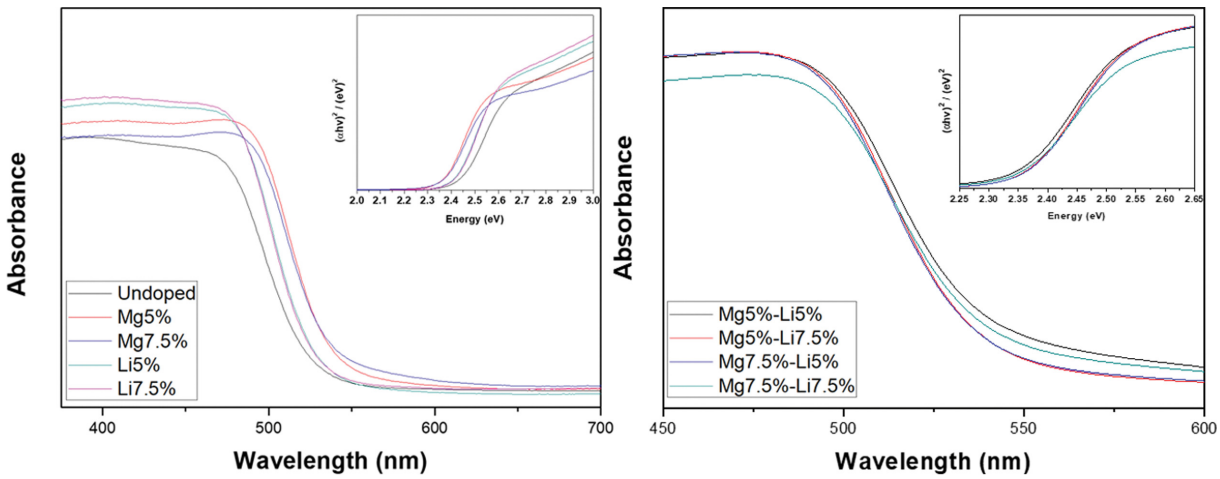

Fig. 3. UV-Vis absorption spectra of the $BiVO_4$ samples. Inset is the plot of $(\alpha h\nu)^2$ vs. energy (hv) of respective samples.

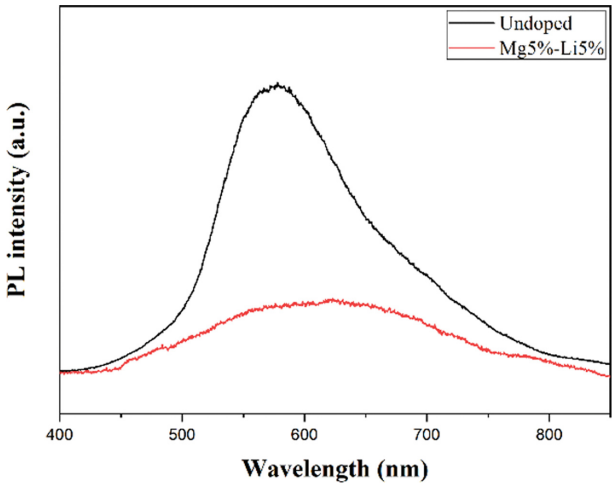

Fig. 4. The comparison of photoluminescence emission spectra of undoped sample and Mg5%-Li5% doped sample.

PL intensity indicates high ability of photo-induced electron-hole pairs separation and, therefore, photocatalytic activity is higher [27]. Figure 4 shows a comparison of the PL emission spectra (blazing wavelength: 300 nm) of the undoped and the Mg5%-Li5% co-doped $BiVO_4$ sample at room temperature. The PL emission spectrum of undoped sample peaks sharply at 580 nm. However, the PL peak of the Mg5%-Li5% co-doped sample nearly disappeared. These results clearly show that Mg5%-Li5% co-doping enhanced the efficiency of photo-induced electron-hole pairs separation, resulting in improved photocatalytic activity.

3.5. Photocatalytic degradation of methyl blue under irradiation with visible light

Figure 5(a, b) presents the time-profiles of the photocatalytic MB degradation under dark and at 405 nm irradiation of the undoped sample, the Mg5%-Li5% co-doped sample and none of catalyst. C_0 represents the initial dye concentration, while C_t represents the dye concentration at a specific time point, t. The photocatalytic degradation of MB under dark didn't work both catalyst and none of catalyst. The photocatalytic degradation of MB at 405 nm irradiation by none of catalyst, the undoped sample and the Mg5%-Li5% co-doped sample was 0 %, 60 %, and 90 % in 240 min, respectively. The addition of Mg5%-Li5% co-doping was found to enhance the photocatalytic activity of $BiVO_4$. Depending on the Langmuir-Hinshelwood kinetics model [28], the photocatalytic degradation of dyes can be described by the below first-order kinetics equation:

$$\ln\left(\frac{C_0}{C_t}\right) = kt + A \quad (2)$$

Here, k represents the apparent first-order rate constant and A is a constant. Figure 5(b) shows the kinetic plot of the photocatalytic MB degradation of the undoped sample and the Mg5%-Li5% co-doped sample. The rate constants of the photocatalytic MB degradation were 0.00364 min^{-1} and 0.00906 min^{-1} for the undoped sample and the Mg5%-Li5% co-doped sample, respectively. This means that the photocatalytic efficiency of the Mg5%-Li5% co-doped sample was 2.48 times higher than that of the undoped sample.

4. Conclusions

Doped and undoped $BiVO_4$ samples were success-

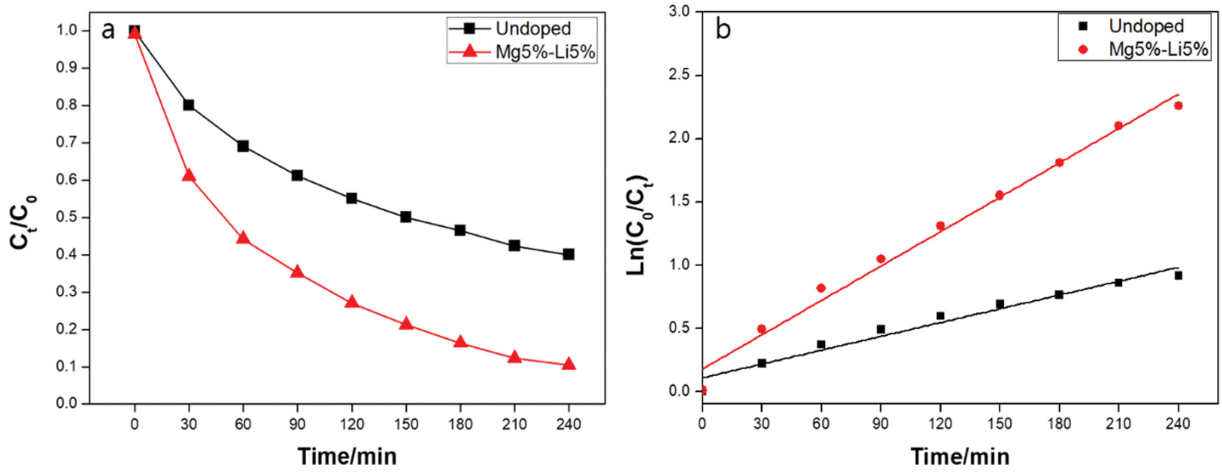

Fig. 5. Photocatalytic MB degradation (a) and the Kinetic plot (b) of undoped sample and Mg5%-Li5% doped sample.

fully synthesized by a hydrothermal method. Mg-doped, Li-doped, and Mg-Li co-doped $BiVO_4$ samples indicated XRD peak shifts due to the lattice distortion. The XPS spectra of the Mg-Li co-doped samples detected surface hydroxyl groups. The UV-Vis spectra of the Mg-Li co-doped samples exhibited a red shift and lowest band gap energy. The PL emission spectra of the undoped sample peaked sharply at 580 nm. However, the PL peak of Mg5%-Li5% co-doped sample was greatly reduced in intensity. Additionally, the photocatalytic degradation of MB under irradiation with visible light showed that the photocatalytic efficiency of Mg5%-Li5% co-doped sample was 2.48 times higher than that of the undoped sample. The results demonstrated that the co-doping of Mg and Li into $BiVO_4$ induced lattice distortion, surface hydroxyl groups, narrowed the band gap, and reduced the recombination rate of photo-induced electron-hole pairs. The co-doped Mg5%-Li5% $BiVO_4$ exhibited significantly enhanced photocatalytic activity compared to the undoped $BiVO_4$, highlighting a remarkable improvement.

References

[1] S. Sun and W. Wang, "Advanced chemical compositions and nanoarchitectures of bismuth based complex oxides for solar photocatalytic application", RSC Adv. 4 (2014) 47136.

[2] J.R. Ran, J. Zhang, J.G. Yu, M. Jaroniecc and S.Z. Qiao, "Earth-abundant cocatalysts for semi-conductor-based photocatalytic water splitting", Chem. Soc. Rev. 43 (2014) 7787.

[3] K. Woan, G. Pyrgiotakis and W. Sigmund, "Photocatalytic carbon-nanotube-TiO_2 composites", Adv. Mater. 21 (2009) 2233.

[4] R. Venkatesan, S. Velumani and A. Kassiba, 'Mechanochemical synthesis of nanostructured $BiVO_4$ and investigations of related features", Mat. Chem. Phys. 135(2-3) (2012) 842.

[5] A. Kudo and Y. Miseki, "Heterogeneous photocatalyst materials for water splitting", Chem. Soc. Rev. 38 (2009) 253.

[6] Y. Hu, J. Fan, C. Pu, H. Li, E. Liu and X. Hu, "Facile synthesis of double cone-shaped $Ag_4V_2O_7/BiVO_4$ nanocomposites with enhanced visible light photocatalytic activity for environmental purification", J. Photochem. Photobiol. A 337 (2017) 172.

[7] M. Guo, Y. Wang, Q. He, W. Wang, W. Wang, Z. Fu and H. Wang, "Enhanced photocatalytic activity of S-doped $BiVO_4$ photocatalysts", RSC Adv. 5 (2015) 58633.

[8] M. Wang, Y. Che, C. Niu, M. Dang and D. Dong, "Effective visible light-active boron and europium co-doped $BiVO_4$ synthesized by sol-gel method for photo-degradion of methyl orange", J. Hazard. Mater. 262 (2013) 447.

[9] S.P. Berglund, A.J.E. Rettie, S. Hoang and C.B. Mullins, "Incorporation of Mo and W into nanostructured $BiVO_4$ films for efficient photoelectrochemical water oxidation", Phys. Chem. Chem. Phys. 14 (2012) 7065.

[10] W.J. Yin, S.H. Wei, M.M. Al-Jassim, J. Turner and Y. Yan, "Doping properties of monoclinic $BiVO_4$ studied by first-principles density-functional theory", Phys. Rev. B83 (2011) 155102.

[11] Z. Zhao, Z. Li and Z. Zou, "Electronic structure and optical properties of monoclinic clinobisvanite $BiVO_4$", Phys. Chem. Chem. Phys. 13 (2011) 4746.

[12] P. Wood and F.P. Glasser, "Preparation and properties of pigmentary grade $BiVO_4$ precipitated from aqueous solution, Ceram. Int. 30 (2004) 875.

[13] J.B. Liu, H. Wang, S. Wang and H. Yan, "Hydrothermal preparation of $BiVO_4$ powders", Mater. Sci. and Eng., B 104 (2003) 36.

[14] L. Shan and Y. Liu, "Er^{3+}, Yb^{3+} doping induced core-shell structured $BiVO_4$ and near-infrared photocatalytic properties", J. Mol. Catal. A Chem. 416 (2016) 1.

[15] J. Tian, Y. Sang, G. Yu, H. Jiang, X. Mu and H. Liu, "A Bi_2WO_6-based hybridphotocatalyst with broad spectrum photocatalytic properties under UV visible, and near-infrared irradiation", Adv. Mater. 25 (2013) 5075.

[16] C. Hu, H. Xu, X. Liu, F. Zou, L. Qie, Y. Huang and X. Hu, "VO_2/TiO_2 nanosponges asbinder-free electrodes for high-performance supercapacitors", Sci. Rep. 5 (2015) 16012.

[17] Y. Zhao, C. Li, X. Liu, F. Gu, H.L. Du and L. Shi, "Zn-doped TiO_2 nanoparticles with high photocatalytic activity synthesized by hydrogen-oxygen diffusion flame", Appl. Catal. B: Environ. 140 (2008) 208.

[18] J. Li, Y. Liu, Z. Zhu, G. Zhang, T. Zou, Z. Zou, S. Zhang, D. Zeng and C. Xie, "A full-sunlight-driven photocatalyst with super long-persistent energy storage-ability", Sci. Rep. 3 (2013) 2409.

[19] Q. Yu, L.A. Li, H.D. Li, S.Y. Gao, D.D. Sang, J.J. Yuan and P.W. Zhu, "Synthesis and properties of boron doped ZnO nanorods on silicon substrate by low-temperature hydrothermal reaction", Appl. Surf. Sci. 257 (2011) 5984.

[20] K. Ding, B. Chen, Z. Fang and Y. Zhang, "Density functional theory study on the electronic and optical properties of three crystalline phases of $BiVO_4$". Theor. Chem. Acc. 132 (2013) 1.

[21] J. Ma and L.-W. Wang, "The role of the isolated 6s states in $BiVO_4$ on the electronic and atomic structures", Appl. Phys. Lett. 105 (2014) 172102.

[22] W.J. Jo, J.W. Jang, H.J. Kang, J.Y. Kim, H. Jun, K.P.S. Parmar and J.S. Lee, "Phosphate doping into monoclinic $BiVO_4$ for enhanced photoelectrochemical water oxidation activity", Angew. Chem. 124 (2012) 3201.

[23] S. Gu, W. Li, F. Wang, H. Li and H. Zhou, "Lanthanide ions Ce(III,IV) substituted for Bi in $BiVO_4$ and its enhanced impact on visible light-driven photocatalytic activities", Catal. Sci. Technol. 6 (2016) 1870.

[24] R. Asahi, T. Morikawa, T. Ohwaki. K. Aoki and Y. Taga, "Visible-light photocatalysis in nitrogen-doped titanium oxides", Science 293 (2001) 269.

[25] A. Galembeck and O. L. Alves, "$BiVO_4$ thin film preparation by metalorganic decomposition", Thin Solid Films. 365 (2000) 90.
[26] J.W. Tang, Z.G. Zou and J.H. Ye, "Photophysical and photocatalytic properties of $AgInW_2O_8$", J. Phys. Chem. B 107 (2003) 14265.
[27] H. Xu, H.M. Li, C.D. Wu, J.Y. Chu, Y.S. Yan and H.M. Shu, "Preparation, characterization and photocatalytic activity of transition metal-loaded $BiVO_4$", Mater. Sci. Eng. B 147 (2008) 52.
[28] R.A. Rajadhyaksha, K. Vasudeva and L.K. Doraiswamy, "Effectiveness factors in Langmuir-Hinshelwood and general order kinetics", J. Catal. 7 (1976) 61.